Cerebral Cortex, May 2019;29: 1851–1865

doi: 10.1093/cercor/bhy042
Advance Access Publication Date: 23 February 2018
Original Article

ORIGINAL ARTICLE

GSK3β Modulates Timing-Dependent Long-Term Depression Through Direct Phosphorylation of Kv4.2 Channels

Giuseppe Aceto[1], Agnese Re[2], Andrea Mattera[1], Lucia Leone[1,5], Claudia Colussi[2], Marco Rinaudo[1], Federico Scala[3], Katia Gironi[1], Saviana Antonella Barbati[1], Salvatore Fusco[1,5], Thomas Green[4], Fernanda Laezza[4], Marcello D'Ascenzo[1,5] and Claudio Grassi[1,5]

[1]Institute of Human Physiology, Università Cattolica del Sacro Cuore, 00168 Rome, Italy, [2]Institute of Cell Biology and Neurobiology, National Research Council, 00015 Rome, Italy, [3]Department of Neuroscience, Baylor College of Medicine, Houston, TX 77030, USA, [4]Department of Pharmacology and Toxicology, University of Texas Medical Branch, Galveston, TX 77555, USA and [5]Fondazione Policlinico Universitario A Gemelli, IRCCS, 00168 Rome, Italy

Address correspondence to Marcello D'Ascenzo, Institute of Human Physiology, Università Cattolica del S. Cuore, Largo Francesco Vito 1, 00168 Rome, Italy. Email: marcello.dascenzo@unicatt.it

Abstract

Spike timing-dependent plasticity (STDP) is a form of activity-dependent remodeling of synaptic strength that underlies memory formation. Despite its key role in dictating learning rules in the brain circuits, the molecular mechanisms mediating STDP are still poorly understood. Here, we show that spike timing-dependent long-term depression (tLTD) and A-type K^+ currents are modulated by pharmacological agents affecting the levels of active glycogen-synthase kinase 3 (GSK3) and by GSK3β knockdown in layer 2/3 of the mouse somatosensory cortex. Moreover, the blockade of A-type K^+ currents mimics the effects of GSK3 up-regulation on tLTD and occludes further changes in synaptic strength. Pharmacological, immunohistochemical and biochemical experiments revealed that GSK3β influence over tLTD induction is mediated by direct phosphorylation at Ser-616 of the Kv4.2 subunit, a molecular determinant of A-type K^+ currents. Collectively, these results identify the functional interaction between GSK3β and Kv4.2 channel as a novel mechanism for tLTD modulation providing exciting insight into the understanding of GSK3β role in synaptic plasticity.

Key words: A-type K^+ current, GSK3β, Kv4.2, personalized medicine, somatosensory cortex, spike timing-dependent plasticity

Introduction

Experience-dependent synaptic changes such as long-term potentiation (LTP) and long-term depression (LTD) modify circuitry connectivity in the brain and occur in response of concerted activity of presynaptic and postsynaptic neurons. An attractive mechanism for experience-dependent synaptic changes is spike timing-dependent plasticity (STDP; Feldman 2012). In comparison to standard stimulation protocols for LTP and LTD induction (i.e., high frequency stimulation and prolonged low frequency stimulation, respectively), STDP is dependent on moderate number of

repeated timed activations of presynaptic and postsynaptic neurons. A postsynaptic action potential (AP) that follow a presynaptic AP (and associate EPSP) within the time window of 10 ms results in timing-dependent LTP (tLTP), whereas APs in the reverse order results in timing-dependent LTD (tLTD) (Nevian and Sakmann 2006; Feldman 2012; Froemke 2015). tLTD has been extensively studied at the cortical synapse between layer 4 spiny stellate cells and layer 2/3 pyramidal cells (Bender et al. 2006; Nevian and Sakmann 2006; Corlew et al. 2007; Banerjee et al. 2009; Carter and Jahr 2016). At these synapses tLTD is developmentally regulated and contributes to the formation of receptive fields in the visual, auditory, and somatosensory systems (Bouvier et al. 2015). Despite the importance of STDP in establishing brain connectivity, the molecular pathways mediating these changes are still poorly understood compared with classical LTP and LTD.

One key enzyme in the brain is GSK3, a serine/threonine (ser/thr) kinase that is ubiquitously expressed in eukaryotes (Ali et al. 2001; Kaidanovich-Beilin and Woodgett 2011). This highly evolutionarily conserved enzyme plays a fundamental role in a variety of functions, including cell proliferation and differentiation (Frame and Cohen 2001; Grimes and Jope 2001), cell survival (Takashima et al. 1993; Pap and Cooper 1998) and cell motility (Lucas et al. 1998; Sánchez et al. 2000). Of the 2 mammalian GSK3 isoforms, GSK3α and GSK3β (Woodgett 1990; Boyle et al. 1991) only GSK3β is highly enriched in the brain (Takahashi et al. 1994), where it has been implicated in several central nervous system (CNS) dysfunctions, such as Alzheimer's disease (Hooper et al. 2008; Kremer et al. 2011), schizophrenia (Lovestone et al. 2007; Emamian 2012; Tamura et al. 2016), mood disorders (Jope 2011; Muneer 2017), and addicted behaviors (Miller et al. 2009).

GSK3β isoform has high basal activity (Doble and Woodgett 2003; Beurel et al. 2015), which is modulated through multiple regulatory mechanisms. In particular, several protein kinases such as Akt (Cross et al. 1995), protein kinase C (Goode et al. 1992), and protein kinase A (Fang et al. 2000; Li et al. 2000), phosphorylate GSK3β at serine 9 located at the N-terminus (Grimes and Jope 2001). This modification inhibits GSK3 ability to phosphorylate its substrates (Kockeritz et al. 2006). Although the full range of GSK3β molecular targets is far from being known new evidence indicates that voltage-gated and ligand-gated ion channels mediating intrinsic excitability and synaptic plasticity are substrates of this enzyme (Bradley et al. 2012; Wildburger and Laezza 2012). In this context, it is particularly relevant the role played by GSK3β in N-methyl-D-aspartate receptor (NMDAR)-dependent synaptic plasticity in the hippocampus. In particular, it has been shown that LTP induction requires inhibition of GSK3β through increased Ser-9-phosphorylation, whereas GSK3β activity is required for LTD induction (Peineau et al. 2008). Therefore, GSK3β is a bidirectional regulator of NMDAR-dependent synaptic plasticity (Hooper et al. 2008; Bradley et al. 2012). Additionally, it has been found that the over-activation of GSK3β is responsible for the Aβ-mediated inhibition of hippocampal LTP (Jo et al. 2011).

Building on the growing interest in understanding GSK3β-mediated mechanisms regulating synaptic plasticity in the CNS, we studied the effects of GSK3β modulation on tLTD induction at the vertical layer 4 input onto layer 2/3 pyramidal neurons in mouse somatosensory cortex. In this brain region GSK3 is highly expressed (Lee et al. 2006). However, the pathophysiological consequences of its activation/inactivation are almost unknown. Although the L4–L2/3 and L2/3–L2/3 synapses represent the major sites of intracortical processing for inputs arriving from thalamic relays, we focused on vertical excitatory inputs onto layer 2/3 neurons because these synapses, in mouse barrel cortex, appear to be more crucial in cortical map plasticity and development (Feldman and Brecht 2005; House et al. 2011). We found that tLTD is modulated by either pharmacological agents or in vivo GSK3β silencing. Moreover, we demonstrate that these effects are mediated by Kv4.2 channel modulation through direct phosphorylation of the Kv4.2 subunit at Ser-616.

Materials and Methods

Ethical Approval

All animal procedures were approved by the Ethics Committee of the Catholic University and complied with Italian Ministry of Health guidelines and with national laws (Legislative decree 116/1992) and European Union guidelines on animal research (No. 86/609/EEC).

Slices Preparation and Electrophysiology

Thalamocortical slices (300 μm) containing the barrel subfield of somatosensory cortex were prepared as previously described (Agmon and Connors 1991). Briefly, C57/BL/6J mice (P15-21) were euthanized by cervical dislocation and decapitated. The brains were rapidly removed and placed in ice-cold, sucrose-based cutting solution containing the following (in mM): Tris–HCl 72, TRIZMA base 18, NaH_2PO_4 1.2, $NaHCO_3$ 30, KCl 2.5, glucose 25, HEPES 20, $MgSO_4$ 10, Na-pyruvate 3, ascorbic acid 5, $CaCl_2$ 0.5, sucrose 20. Thalamocortical slices (300 μm thick) were cut on a vibratome (VT1200S; Leica Microsystems, Germany) and immediately transferred to an incubation chamber held at 32 °C and filled with a recovery solution containing (in mM): TRIS-HCl 72, TRIZMA base 18, NaH_2PO_4 1.2, $NaHCO_3$ 25, KCl 2.5, glucose 25, HEPES 20, $MgSO_4$ 10, Na-pyruvate 3, ascorbic acid 5, $CaCl_2$ 0.5, sucrose 20. After 30 min, thalamocortical slices were transferred to a second incubation chamber held at 32 °C and filled with artificial cerebrospinal fluid (aCSF) containing the following (in mM): NaCl 124, KCl 3.2, NaH_2PO_4 1.2, $MgCl_2$ 1, $CaCl_2$ 2, $NaHCO_3$ 26, and glucose 10, pH 7.4. During incubations, the chambers were continuously bubbled with 95% O_2/5% CO_2. Finally, slices were equilibrated at RT for at least 45 min. For electrophysiological recordings, slices were transferred to a submerged recording chamber constantly perfused with heated aCSF (32 °C) and bubbled with 95% O_2/5% CO_2. Neurons of the layer 2/3 area were visualized under DIC infrared illumination. Stimulation at the base of a layer 4 barrel was obtained by means of a current stimulus isolator (WPI, USA), connected to a bipolar concentric stimulating electrode (FHC, USA). Patch pipettes had a resistance of 4–6 MΩ when filled with an internal solution containing (in mM): K-gluconate 145, $MgCl_2$ 2, HEPES 10, EGTA 0.1, Na-ATP 2.5, Na-GTP 0.25, phosphocreatine 5, pH adjusted to 7.2 with KOH.

Recordings were performed using a Multiclamp 700B/Digidata 1550A system (Molecular Devices, USA) and digitized at a 10 000 Hz sampling frequency. All the electrophysiological recordings were analyzed using the Clampfit 10.6 software (Molecular Devices). Only cells with a stable resting membrane potential negative to −60 mV, overshooting APs (exceeding 75–80 mV threshold-to-peak) and an input resistance >100 MΩ were included. Furthermore, cells were rejected if resting membrane potential and input resistance changed by more than 20%. Excitatory postsynaptic potentials were recorded in whole-cell, current-clamp mode from layer 2/3 pyramidal neurons in mouse barrel cortex. Neurons were held to −70 mV by

passage of direct current with the patch amplifier. Baseline EPSPs were recorded for 10 min at 0.2 Hz stimulation. Then EPSPs were paired with 3 APs at 100 Hz elicited by brief somatic current injections (1–2 nA; 1 ms). In particular, a post-before-pre pairing protocol ($\Delta t = -10$ ms) were applied 60 times at 0.1 Hz. In a subset of experiments EPSPs were paired with a single AP. Inhibitory inputs were not blocked using $GABA_A$ blockers. The change in EPSP slope was evaluated 35–40 min after the end of the pairing period and normalized to the baseline EPSP slope. The slope of the EPSP was measured as a linear fit between time points on the rising phase of the EPSP corresponding to 25% and 75% of the peak amplitude during control conditions.

The transient A-type K^+ current in voltage–clamp mode was recorded by applying 400 ms voltage step from −110 to +40 mV. Prepulse of hyperpolarization at −110 mV for 100 ms removed A-Type K^+ channel inactivation and enables subsequent maximum activation. The transient channel was inactivated by the same voltage steps preceded by a depolarizing prepulse of −10 mV for 100 ms, leaving the sustained current of the total outward current. The transient current was then isolated by a digital subtraction of the sustained current from the total outward current. To record A-type K^+ current the following reagents were added to the external solution: 1 μM tetrodotoxin (TTX); 300 μM Cd^{2+} and 20 mM of tetraethylammonium (TEA). Excitatory and inhibitory synaptic transmission were also blocked using NBQX (10 μM) and picrotoxin (50 μM). Data obtained from a given cell were rejected if series resistance (Rs) was larger than 40 MΩ or changed by >20% during the course of the experiment. Current densities were obtained by dividing A-type K^+ current amplitude by membrane capacitance. Membrane capacitance was calculated using the equation: capacitance = membrane time constant/input resistance (Meitzen et al. 2009). The membrane input resistance was measured by a series of 600 ms hyperpolarizing current steps from −50 to 0 pA, step 10 pA with 1 s interval. The slope of the current–voltage curve is designated as the membrane input resistance. The membrane time constant was calculated by fitting a single exponential curve to the membrane potential change in response to −200 pA hyperpolarizing pulses. Biocytin immunohistochemistry was performed according to previously described methods (Jiang et al. 2015). Briefly, after recording experiments, the slices were fixed by immersion in freshly prepared 2.5% glutaraldehyde/4% paraformaldehyde in 0.1 M phosphate-buffered saline at 4° for at least 48 h. The slices were subsequently processed with the avidin–biotin–peroxidase method in order to reveal the morphology of the neurons. The morphologically recovered cells were examined using a ×100 oil-immersion objective lens and a camera lucida system.

Immunohistochemistry and Confocal Microscopy Analysis

Mice were anesthetized with a cocktail of ketamine (100 mg/mL) and xylazine (1 mg/mL) and transcardially perfused with Ringer's solution followed by 4% paraformaldehyde fixative solution. The brains were removed, post-fixed overnight at 4 °C, cut with a vibratome (Leica VT 1200S) in to coronal sections (30-μm-thick) and floated in ice-cold PBS. Sections were blocked for 45 min at RT in 1% bovine serum albumin (BSA) solution containing 10% goat serum and 0.5% Triton X-100 (Sigma-Aldrich).

Immunodetection of GSK3β and kcnd2 (i.e., Kv4.2) was performed in sections after antigen retrieval in 0.01 M citrate buffer at 95 °C for 5 min. Brain sections were then permeabilized and blocked in 0.5% triton/10% BSA in PBS for 1 h and primary antibodies (anti-GSK3β polyclonal, Cell signalling Technology; 1:400) (anti-kcnd2 monoclonal Origene, 1:200) were added in a solution of 0.2% triton/5% BSA in PBS for 48 h. After 3 washes in PBS, secondary antibodies were added for 1 h and nuclei counterstained with DAPI for 20 min. Z-stacked images of the 2 proteins were acquired with a Nikon-Ti Eclipse equipped with a ×60 objective. Colocalization analysis was performed with Image j-WCFI software and Pearson's correlation (Rr), Manders' overlap coefficient (R) and red–green correlation plot were generated.

Virus Injection

Adeno-associated viral vector (AAV2) which uses RNA interference to knockdown GSK3β (AAV-shGSK3β) and control vector (AAV-shCTRL) used in this study were previously constructed and validated (Crofton et al. 2017). Viral injections were performed according to previous studies (Bovetti et al. 2017). Briefly, pups between p1 and p3 (considering p0 as the day of birth) were anesthetized using hypothermia, placed on a stereotaxic apparatus and kept at approximately 4 °C until the end of the surgery. The skull was exposed through a small incision in the skin and ~300 nL of viral solution were slowly injected using a glass micropipette at stereotaxic coordinates of 0 mm from bregma, 1.5 mm lateral of the sagittal sinus and 0.1–0.2 mm depth. As confirmed by our immunohistochemical and electrophysiological experiments and data taken from literature, these coordinates coincided with the somatosensory area of the neocortex (Zucca et al. 2017). Following injection the micropipette was held in place for 2 min and was retracted slowly, in order to avoid spillage of the viral solution outside the skull. After pipette removal, the skin was sutured and the pup was revitalized on a heating pad. Before being reintroduced in the nest, pups were gently rubbed with bedding from the home cage in order to remove possible adverse odor acquired during surgical procedure. Pups were then reintroduced in the nest within the home cage with their mother and were monitored daily. Each procedure lasted less than 10 min. To avoid distressing the mother, only one pup at time was taken from the cage for the procedure. Electrophysiological recordings were made after 15–18 days in pyramidal neurons expressing GFP only in layer 2/3 somatosensory cortex.

Electrophysiology on HEK293 Expressing Kv4.2 Construct

Cell culture was carried out using standard procedures. HEK-293 cells were maintained in DMEM supplemented with 10% fetal calf serum (GIBCO BRL) and incubated in a humidified atmosphere containing 5% CO_2 in air at 37 °C. pEGFP Kv4.2or pEGFP Kv4.2 ($Kv4.2^{S616A}$) vectors (1 μg each) mutated at Ser-616 were transfected into HEK293 cells using polyethyleneimine (PEI; Polysciences, Eppelheim, Germany) according to manufacturer's instruction. The pEGFP Kv4.2 was kindly provided by Dr. Dax Hoffman (National Institutes of Health, Bethesda, USA). All experiments were performed on HEK293 cells within 20 passages. Electrophysiological experiments were performed in HEK293 cells 24 h after transfection.

Kv4.2-mediated K^+ currents were studied using the whole-cell patch-clamp technique in voltage-clamp configuration. Experiments were carried out at room temperature (22–25 °C) by using a MultiClamp-700B amplifier and Digidata-1440A A/D converter (Axon Instruments, CA, USA). Recording electrodes were pulled using a Sutter P-97 puller (Sutter Instruments, CA,

USA). Electrodes were filled with intracellular solution containing (in millimolar): 125 KCl, 4 $MgCl_2$, 10 HEPES, 10 EGTA, and 5 MgATP, adjusted to 310 mOsm/L with sucrose, pH 7.2 with KOH. The external solution contained (in millimolar): 141 NaCl, 4.7 KCl, 1.2 $MgCl_2$, 1.8 $CaCl_2$, 10 glucose, and 10 HEPES, adjusted to 330 mOsm/L with sucrose, pH 7.4 with NaOH. The resistance of the recording pipette filled with internal solution was 4–6 MΩ. The adjustment of capacitance compensation and series resistance compensation was done before recording the membrane currents. The holding potential was −60 mV. Membrane currents were filtered at 1 kHz and digitized at 10 kHz, and the data were stored in compatible PC computer for off–online analysis using the pCLAMP 10 acquisition software (Axon Instruments, CA, USA). The voltage-dependence of activation was studied by a 400 ms constant depolarizing pulse from −90 to +40 mV in 10 mV steps (see Supplementary Fig. S4). To determine the voltage-dependence of steady-state inactivation of Kv4.2, the voltage-dependence of inactivation was assessed by measuring the peak amplitude of current responses evoked by test depolarization to +40 mV after 1.5 s prepulse to potentials between −110 and 0 mV with 10 mV increment (see Supplementary Fig. S4).

Coimmunoprecipitation

HEK293 cells were transfected with Kv4.2-EGFP or the empty EGFP vectors and lysed after 36 h with a buffer containing 0,15 M NaCl, 50 mM Tris HCl pH 7.4, 1% NP-40 and protease inhibitors. Samples were quantified and diluted to the same amount. Immunoprecipitation was carried out by incubating the samples overnight with end-over-end rotation at 4 °C with antibody against GSK3β (Cell Signaling 12 456). Protein A-coupled agarose beads were incubated with the sample for 3 h, then immunocomplexes bound to the beads were isolated by 500 × *g* centrifugation and washed 5 times. Pellet was resuspended in laemmli buffer and loaded on 8% polyacrilammide gel. After blotting, the membranes were exposed to antibodies against GSK-3β (Cell Signaling 12 456) or against EGFP (Invitrogen A11122).

Tissue extracted from somatosensory cortex was homogenized in lysis buffer, gently sonicated and centrifugated 2 times at 14 000 × *g* to remove debris. The supernatant was split in 2 and one half was incubated with antibody against GSK-3β, whereas the other half was incubated with IgG as negative control. Samples were incubated overnight with antibody with end-over-end rotation at 4 °C. Protein A-coupled agarose beads were pretreated with 0,5% BSA overnight with end-over-end rotation at 4 °C to block aspecific sites, then washed 3 times with lysis buffer and incubated with the sample for 3 h. Immunocomplexes bound to the beads were isolated by 500 × *g* centrifugation and washed 5 times. Pellet was resuspended in laemmli buffer and loaded on 8% polyacrilammide gel. After blotting, the membranes were exposed to antibodies against GSK-3β (Cell Signaling 12 456) or against Kv4.2 (Abcam ab99040).

Western-Blot Assay

Protein extracts from HEK293 cells were obtained with USA Buffer (Tris-Hcl 50 mM pH7.5; EDTA 5 mM; NaCl 250 mM; EGTA 1 mM, Triton 0.1%; NaF 50 mM) (Re et al. 2016). The 50 μg of total extract were resolved by SDS-PAGE using a 3–8% gradient (Invitrogen, NuPage and SDS buffer) or 7.5% Precast gel (Biorad). Specific protein signals were revealed with ECL Prime (Amersham, GE Healthcare) and detected by UVIDOC (Eppendorf S.r.l.). The intensity of each band was evaluated by using UVIDOC. Antibodies: Anti-Kv4.2 (S57-1, Abcam), anti-Kv4.2/KCND2 (Phospho-Ser616, MyBioSource), Anti-GAPDH (6C5, Abcam), Anti-βActina (Abcam).

Single Cell Reverse Trascription Quantitative Real-Time PCR

GSK3β gene expression in single pyramidal neurons of somatosensory cortex brain slices was assessed by single cell real-time RT-PCR. Single cell contents from pyramidal neurons were collected as previously described (Jiang et al. 2013; Cadwell et al. 2016). Briefly, presterilized glass electrodes were filled with Rnase-free intracellular solution containing 1 U/μL recombinant Rnase inhibitor (Ambion) and then used to obtain whole cell patches on pyramidal neurons in somatosensory brain cortex slices. The intracellular contents (~4–5 μL) were drawn into the tip of the patch pipette by applying negative pressure and were then transferred to RNase/DNase-free tubes. The volume in each tube was brought up to 10 μL by adding Single Cell DNase I/Single Cell Lysis solution of Ambion Single Cell-to-CT kit (Life Technologies, Grand Island, NY), and then the contents were incubated at room temperature for 5 min. Following cDNA synthesis by performing reverse transcription in a thermal cycler (25 °C for 10 min, 42 °C for 60 min, and 85 °C for 5 min), GSK3β gene expression primers were mixed with preamplification reaction mix based on the instructions from the kit (95 °C for 10 min, 14 cycles of 95 °C for 15 s, 60 °C for 4 min, and 60 °C for 4 min). The products from the preamplification stage were used for the Real-time qPCR reaction (50 °C for 2 min, 95 °C 10 min, and 40 cycles of 95 °C for 5 s and 60 °C for 1 min) on Applied Biosystems 7500 thermocycler with validated primers and probe designed to detect mouse GSK3β. GSK3β mRNA levels were normalized to the housekeeping gene Hprt and analyzed by using the $2^{-\Delta\Delta Ct}$ method. Single cell qPCR products were also separated by electrophoresis on a 3% agarose gel containing 1 μL/mL ethidium bromide.

Statistical Analysis

Data are expressed as means ± standard errors of the means (SEM). Statistical significance was assessed with either Student's *t* test and one-way ANOVA for multiple groups comparison (with Tukey post hoc test). Statistical analysis was performed with SYSTAT 10.2 software (Statcom, Inc., Richmond, CA). The level of significance was set at 0.05.

Results

tLTD at L4-L2/3 Synapses

Electrophysiological recordings in acute slices of the mouse somatosensory cortex were performed with the whole-cell patch-clamp technique from visually identified layer 2/3 pyramidal neurons. In addition to morphological criteria (pyramidal soma shape), neurons were identified based on previously defined electrophysiological parameters (Connors and Gutnick 1990; Agmon and Connors 1992; Feldman 2000). In some experiments cells were filled with biocytin and anatomically reconstructed for further validation (Fig. 1*A*,*B*). Excitatory postsynaptic potentials (EPSPs) were evoked using extracellular stimulation in layer 4 of the same barrel column and recorded at a frequency of 0.2 Hz. After a 10 min control period, EPSPs were paired (60 times at 0.1 Hz) with a postsynaptic burst of APs (APs) consisting of 3 spikes delivered at 100 Hz followed by an EPSP evoked with a 10 ms delay (Fig. 1*C*). After pairing, EPSPs slope gradually

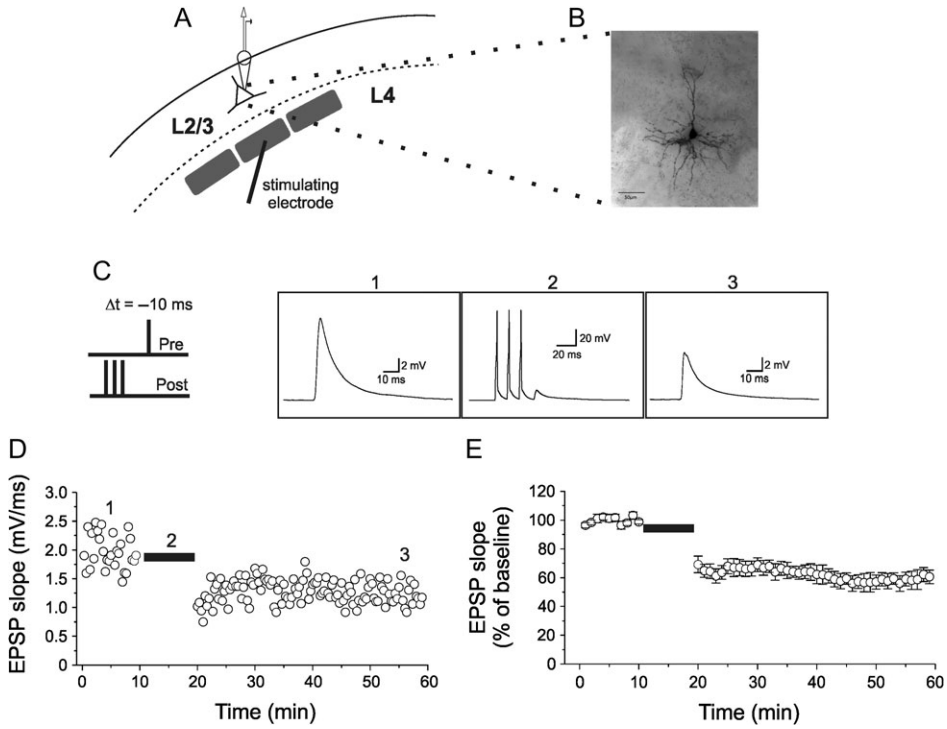

Figure 1. Timing-dependent induction of LTD by pairing an EPSP and a short burst of APs in layer 2/3 pyramidal neurons in the mouse somatosensory cortex. (*A*) Schematic diagram of a layer 2/3 pyramidal neuron with patch pipette located in the soma and stimulating electrode at the base of a layer 4 barrel. (*B*) Z-stack acquisition of morphological recovered pyramidal neurons within the layer 2/3 in the mouse somatosensory cortex. (*C*) The induction protocol for t-LTD is depicted on the left. A short burst of 3 APs at 100 Hz, elicited by current injections into the postsynaptic neuron (post), was paired with a following EPSP evoked by extracellular stimulation (pre). The last AP in the burst preceded the onset of EPSP by $\Delta t = -10$ ms. To the right, representative traces of evoked EPSP in control (1), during pairings with a burst of APs (2) and after conditioning (3). (*D*) EPSP slope for the entire experiment. The burst-pairing period is indicated by a horizontal black bar. The representative traces shown in C are taken from the episodes indicated by corresponding numbers in *D*. (*E*) Normalized mean ± SEM for 10 experiments (from 5 mice). In all experiments resting membrane potentials and input resistance did not change by >30%.

reaching a steady-state amplitude of 59.7 ± 1.8% compared with control (Fig. 1*D*,*E*; mean ± SEM; $n = 10$). EPSP slope depression lasted through the recording session (~40 min) and was ascribed as timing-dependent LTD (tLTD) in accordance to previous studies (Bender et al. 2006; Nevian and Sakmann 2006; Rodríguez-Moreno and Paulsen 2008; Rodríguez-Moreno et al. 2010; Banerjee et al. 2014). Furthermore, tLTD was also induced by pairing a single AP with an EPSP ($\Delta t = -10$ ms). In this experimental conditions tLTD was slightly but significantly reduced compared with that observed with burst-firing-associated tLTD (68.6 ± 3.9%; vs. 59.7 ± 1.8%; $n = 9$ and 10, respectively; one-way ANOVA; $F_{(2,19)} = 5.04$; $P < 0.05$; followed by Tukey post hoc test, $P < 0.05$; Supplementary Fig. S1A,B), in accordance to previous observations (Nevian and Sakmann 2006).

GSK3β-Dependent Modulation of tLTD

To determine whether GSK3 is involved in tLTD modulation we tested the effects of the high selective GSK3 inhibitor, CT-99021 (Peineau et al. 2007; Jo et al. 2011; Franklin et al. 2014; Chen et al. 2015; Hsu et al. 2015; Kailainathan et al. 2016) on burst-inducing tLTD. Since it is believed that tLTD is induced and expressed postsynaptically we infused individual layer 2/3 pyramidal neurons with CT-99021 (1 μM) via a whole-cell patch pipette to selectively block GSK3 in the postsynaptic cell. Under these experimental conditions tLTD was significantly increased compared with what observed when vehicle (DMSO; 1/1000 dilution) was intracellularly perfused (one-way ANOVA; $F_{(2,29)} = 11.69$; $P < 0.001$; followed by Tukey post hoc test, $P < 0.05$; Fig 2*A*,*B*). tLTD was 43.7 ± 5.3% of baseline value in pyramidal neurons intracellularly perfused with CT-99021 ($n = 9$) and 62.2 ± 4.4% in vehicle-treated neurons ($n = 11$).

GSK3 activity is normally suppressed by its N-terminal phosphorylation at Ser-9 induced by protein kinase B type 1 (Akt-1) (Emamian et al. 2004; Jo et al. 2011). We therefore speculated that pharmacological inhibition of Akt-1 would lead to reduced tLTD through an increased GSK3β activation. In support of this hypothesis we found that when the Akt-1 inhibitor triciribine (10 μM) was intracellularly perfused into pyramidal neurons the tLTD was significantly reduced compared with control experiments (Fig. 2*A*,*B*; 79.6 ± 6.7% of baseline value; $n = 9$; one way ANOVA; $F_{(3,29)} = 11.69$; $P < 0.001$ followed by Tukey post hoc test, $P < 0.05$). Correlation between tLTD magnitude and GSK3 activity strongly suggest that this enzyme is critically involved in tLTD modulation at layer 4-to-layer 2/3 connection of primary somatosensory cortex.

To further validate the specific role of the GSK3β isoform in establishing the observed phenotype we used in vivo genetic silencing achieved through an adeno-associated viral vector (AAV2) short hairpin RNA against mouse GSK3β (AAV-shGSK3β-GFP; Crofton et al. 2017). As control experiment we used a validated AAV-shCTRL-GFP that does not target any known mouse transcripts (Benzon et al. 2014; Crofton et al. 2017). AAV-shGSK3β-GFP vector was validated, in our experimental conditions, by in vivo injecting AAV-shGSK3β-GFP or AAV-shCTRL-GFP into the layer 2/3 somatosensory cortex of newborn mice (P0–2) and comparing the amount of GSK3β mRNA at P15–21 days using a recent developed protocol that combines whole-cell patch-clamp

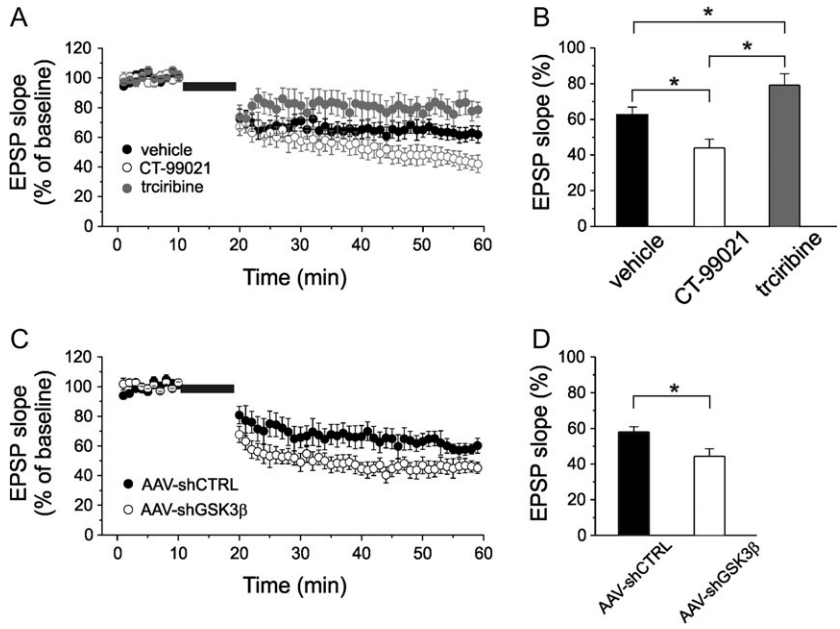

Figure 2. The modulation of GSK3β affects tLTD. (*A*) Time course of EPSP slope, normalized to baseline values, during tLTD experiments in which vehicle (black circle; $n = 11$ cells from 6 mice), CT-99021 (1 μM; open circle; $n = 9$ cells from 5 mice) or triciribine (10 μM; gray circle; $n = 9$ cells from 5 mice) were intracellularly perfused through the patch-pipette. (*B*) Bar graph comparing the average EPSP slope measured during the last 5 min recording expressed as a percentage of the baseline slope (100%) under the experimental conditions shown in A. (*C*) tLTD was significantly increased in pyramidal neurons transfected with a vector designed to knockdown GSK3β (AAV-shGSK3β; open circle; $n = 9$ cells from 6 mice) compared with tLTD measured in pyramidal neurons transfected with control vector (AAV-shCTRL; black circle; $n = 9$ cells from 6 mice). Note that the magnitude of AAV-shCTRL tLTD was comparable to vehicle tLTD showed in panels *A* and *B*. (*D*) Bar graph comparing the average EPSP slope in the experimental conditions reported in *C*.

recordings with high-quality single cell reverse transcription quantitative real-time PCR (Jiang et al. 2013; Cadwell et al. 2016). As shown in supplementary figure 2, the amount of GSK3β mRNA was reduced by ~70% in pyramidal neurons where shRNA construct was expressed.

We hypothesized that knocking down GSK3β in pyramidal neurons would result in increased tLTD similarly to what observed after pharmacological inhibition of GSK3. As shown in Figure 2*C*,*D*, pairing stimulation-induced tLTD was more pronounced in neurons transfected with AAV-shGSK3β compared with control (one way ANOVA; $F_{(2,18)} = 8.2$; $P < 0.005$; followed by Tukey post hoc test; $P < 0.05$). EPSP slope was 44.3 ± 4.3% of baseline in pyramidal neurons transfected with AAV-shGSK3β-GFP ($n = 9$) and 58.1 ± 2.8% of baseline in AAV-shCTRL-GFP transfected neurons ($n = 9$). Taken together, these results indicate that the levels of active GSK3β isoform inversely regulate tLTD magnitude in somatosensory cortex.

Pharmacological Blockade of A-Type K^+ Channel Mimics Triciribine's Effect on tLTD and Prevents Further Modulation by Triciribine

In a recent study we demonstrated that in hippocampal neurons GSK3-dependent phosphorylation of the Kv4.2 α-subunit, a molecular determinant of A-type K^+ currents, results in a reduction of the channel activity and, as consequence, broadening of AP and increased neuronal firing (Scala et al. 2015). These findings, together with the notion that A-type K^+ channels, beyond their traditional role in regulating AP firing, contribute to the regulation of synaptic strength (Chen et al. 2006; Kim and Hoffman 2008; Yang and Dani 2014), led us to postulate that Kv4.2 could be a downstream target of GSK3β-dependent modulation of tLTD. As weak intracellular Ca^{2+} elevation is required for the induction of tLTD (Feldman 2012; Carter and Jahr 2016; Nevian and Sakmann 2006) we hypothesized that GSK3β-dependent down-regulation of Kv4.2 could lead to broadened dendritic back propagation, increased Ca^{2+} influx during pairing protocol and reduced tLTD.

We first confirmed, in our experimental conditions, the post-synaptic Ca^{2+}-dependency of tLTD by performing a set of experiments in which the calcium chelator BAPTA (10 mM) was infused in pyramidal neurons via the recording pipette. As shown in supplementary figure 3 no modification of the synaptic strength could be observed (102.1 ± 5.1% of baseline value, $n = 8$; $P > 0.001$; one way ANOVA; $F_{(2,18)} = 82.5$; $P < 0.001$ vs. controls). We then examined the effects of 4-aminopyridine (4-AP), an A-type K^+ channel blocker, on tLTD induction. Different 4-AP concentrations have been used to block A-type K^+ channels expressed in various neuronal preparations (Yu et al. 1998; Yang et al. 2001; Duan et al. 2012; Yang and Dani 2014). We added 60 μM of 4-AP to the bath solution because, at this concentration, 4-AP reduces the A-type K^+ current (~30%) to a level that still allows the cell to fire (Ye et al. 2003; Mitterdorfer and Bean 2002; Scala et al. 2015). Under these conditions tLTD was significantly reduced compared with vehicle (Fig. 3*A*,*B*; 76.2 ± 2.7% vs. 62.2 ± 4.4%; one way ANOVA; $F_{(3,36)} = 3.4$; $p < 0.05$; followed by Tukey post hoc test; $P < 0.05$; $n = 8$ and 11, respectively). Interestingly, the magnitude of the inhibitory effect of 4-AP was comparable to that observed upon perfusion with triciribine (76.2 ± 2.7% vs. 79.6 ± 6.7% one way ANOVA; $F_{(3,36)} = 3.4$; $P > 0.05$; followed by Tukey post hoc test; $P > 0.5$), suggesting that the 2 mechanisms might be related. We then hypothesized that if neuron treatment with triciribine involves GSK3-dependent down-regulation of Kv4.2, in an experimental condition in which triciribine and 4-AP were acting together the magnitude of tLTD would not be significantly different from that obtained

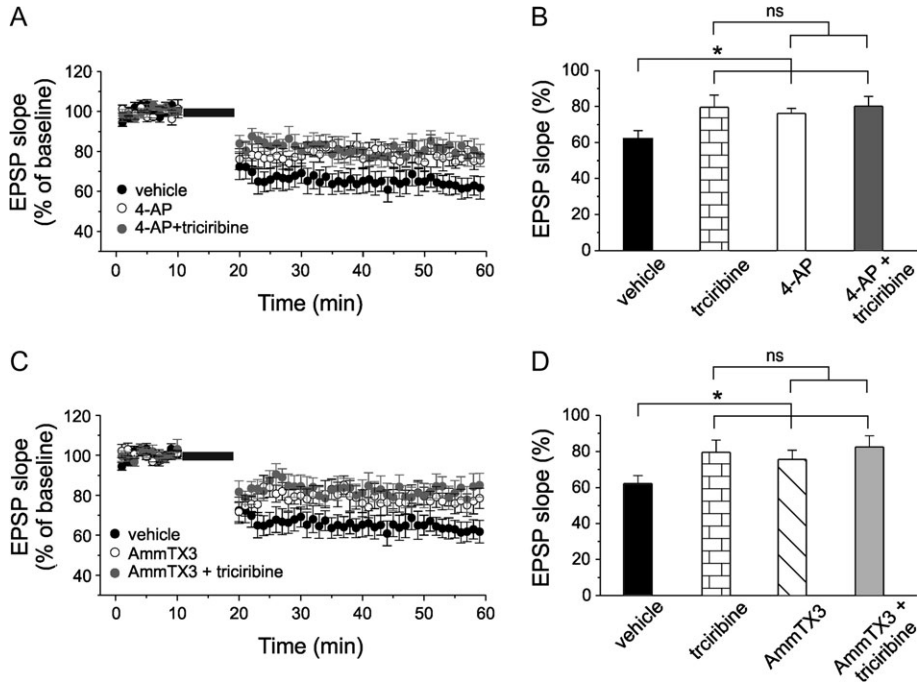

Figure 3. Pharmacological A-type K^+ channels inhibition occludes triciribine's effect on tLTD. (*A*) Average time course of EPSP slope during t-LTD experiments in neurons from slices treated with 60 μM 4-AP (open circle; $n = 8$ cells from 4 mice) and in neurons recorded from slices treated with 4-AP while triciribine was intracellularly perfused (gray circle; $n = 9$ cells from 5 mice). For comparison, vehicle tLTD is also shown (black circle, same recordings shown in Figure 2A). (*B*) Bar graph depicting quantification of tLTD in the experimental conditions reported in the panel *A*. Note that the impairment of tLTD in neurons treated with 4-AP and in neurons treated with 4-AP plus triciribine are comparable to that induced by triciribine alone. (*C*) tLTD was significantly decreased also in neurons from slices treated with 200 nM AmmTX3 (open circle; $n = 10$ cells from 5 mice) and in neurons recorded from slices treated with AmmTX3 while triciribine was intracellularly perfused (gray circle; $n = 10$ cells from 5 mice). (*D*) Bar graph showing that the impairment of tLTD in neurons treated with AmmTX3 and in neurons treated with AmmTX3 plus triciribine are comparable to that induced by triciribine alone.

when triciribine and 4-AP were applied alone. Indeed, tLTD was 80.1 ± 5.5% of baseline value following 4-AP plus triciribine application (Fig. 3A,B; one way ANOVA followed by Tukey post hoc test; $n = 9$; $P > 0.5$). Since 4-AP could affect other K^+ channels besides Kv4.2, such as Kv1 subfamily, we repeated the above experiments using the more selective inhibitor of Kv4.2 channels AmmTX3 (Maffie et al. 2013; Pathak et al. 2016). As shown in Figure 3, when 200 nM of AmmTX3 was present in the bath tLTD was significantly reduced compared with vehicle experiment (Fig. 3C,D; 75.6 ± 5.1% vs. 62.2 ± 4.4%; one way ANOVA; $F_{(3,39)} = 3.1$; $P < 0.05$; followed by Tukey post hoc test; $P < 0.05$; $n = 10$ and $n = 11$, respectively). Furthermore, as expected, AmmTX3 occluded the triciribine's effect on tLTD. Indeed, in an experimental condition in which triciribine and AmmTX3 were coadministrated tLTD was not significantly different from that obtained when either triciribine or AmmTX3 was applied alone (Fig. 3C,D; one way ANOVA followed by Tukey post hoc test; $n = 10$; $P > 0.5$).

Finally, we tested the effect of Dendrotoxin (DTX; 100 nM), a selective inhibitor of Kv1 channels on tLTD. If these channels substantially contribute to the repolarization of APs in layer 2/3 pyramidal neurons we would expect modulation of tLTD by DTX application. However, in accordance to previous observations reporting that APs are partially repolarized by Kv1 channels (Pathak et al. 2016), no difference in tLTD was observed in this experimental condition compared with control experiment (Supplementary Fig. S4; DTX: 63.5 ± 6.2%, $n = 8$; control 59.7 ± 1.8%, $n = 10$; one-way ANOVA; $P > 0.05$). All together these data suggest that modulation of Kv4.2 channels underlies GSK3 action on tLTD.

GSK3β-Dependent Modulation of A-Type K^+ Currents in Layer 2/3 Pyramidal Neurons of Somatosensory Cortex

To strengthen the above evidence we performed whole-cell patch-clamp recordings in voltage-clamp mode and compared the magnitude of A-Type K^+ currents after intracellular perfusion of CT-99021, triciribine and vehicle.

Representative traces of the total outward currents recorded in response to voltage steps from −110 to +40 mV are shown in Figure 4A. A hyperpolarizing prepulse at −110 mV for 100 ms was used to remove A-Type K^+ channel inactivation and enable subsequent maximal channel activation. The same neurons were also subjected to a protocol in which the same voltage steps were preceded by a depolarizing prepulse at −10 mV for 100 ms to inactivate A-type K^+ transient currents and allow isolation of the slowly inactivating currents (Fig. 4B; Hoffman and Johnston 1998; Li et al. 2013; Scala et al. 2015). The transient current was subsequently obtained by digital subtraction (total-sustained, Fig. 4C). When K^+ currents were recorded in the presence of 5 mM 4-AP, the transient currents were completely inhibited thus confirming the A-Type identity of the K^+ currents (data not shown). As shown in Figure 4D,E, intracellular CT-99021 infusion significantly increased A-type K^+ current density compared with vehicles (Fig. 4D,E; CT-99021:13.8 ± 0.9 pA/pF, $n = 27$; vehicle: 10.0 ± 1.3 pA/pF; $n = 21$; one-way ANOVA; $F_{(2,39)} = 12.5$; $P < 0.001$ followed by Tukey post hoc test, $P < 0.05$). Conversely, triciribine had an opposite effect on A-Type K^+ current density (Fig. 4D,E; triciribine: 6.5 ± 0.9 pA/pF; $n = 24$; $F_{(2,39)} = 13.9$; $P < 0.001$ ANOVA followed by Tukey post hoc test, $P < 0.05$). Moreover, in neurons transfected with AAV-shGSK3β a

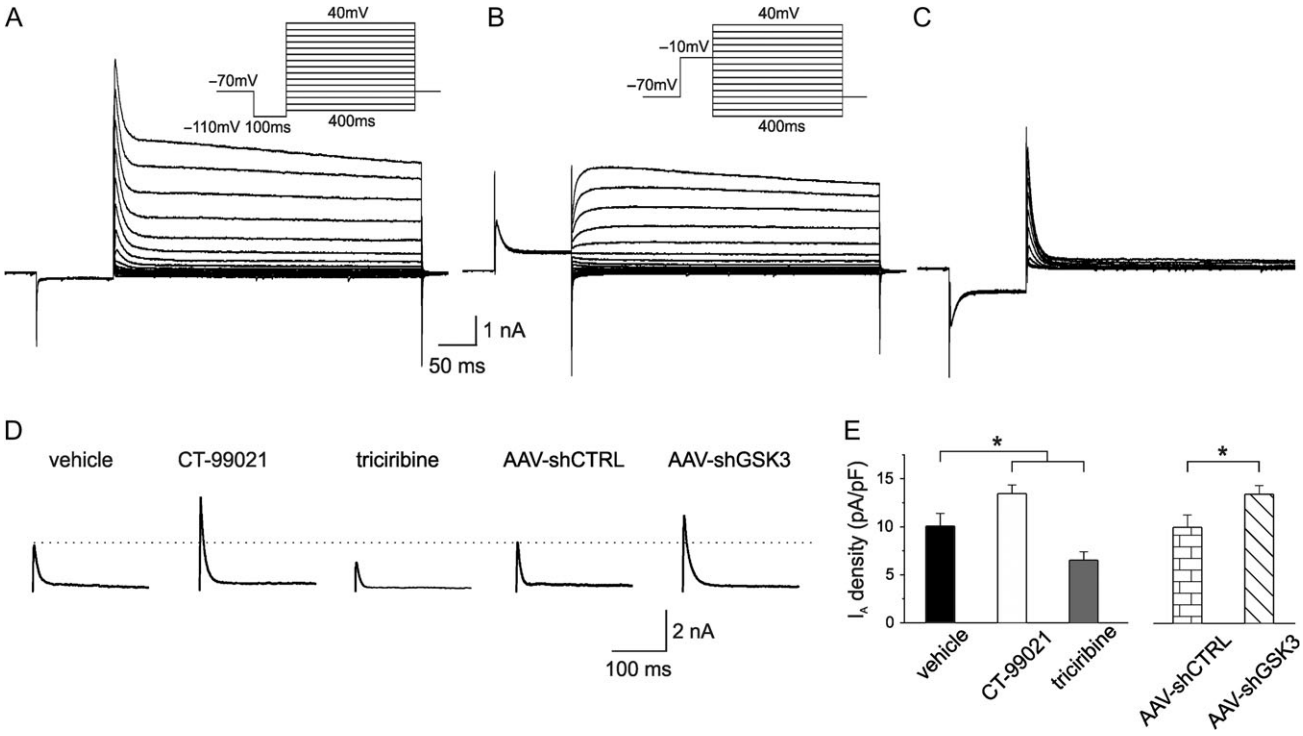

Figure 4. Isolation of A-type K^+ currents in layer 2/3 of somatosensory cortex and its GSK3β-mediated modulation. (*A*) Whole cell voltage-clamp recording of the outward currents evoked by a series of depolarizing steps from −110 to +40 mV following a hyperpolarizing step to −110 mV to enable maximal K^+ conductance (holding potential: −70 mV). Inset: voltage protocols. (*B*) To inactivate the transient K^+ channels a prepulse to −10 mV (100 ms) was applied before the voltage steps. Inset: voltage protocols. (*C*) The transient A-type K^+ currents were isolated by digital subtracting the currents in panel *B* from those in panel *A*. The recordings of isolated A-type K^+ currents in pyramidal neurons were obtained after 10 min perfusion of ACSF containing 1 μM TTX, 300 μM Cd^{2+} and 20 mM of TEA. (*D*) Representative traces showing transient A-type K^+ currents recorded at +40 mV upon intracellular perfusion of vehicle (left), CT-99021, triciribine, AAV-shCTRL and AAV-shGSK3β. (*E*) Graph showing A-type K^+ current densities under the experimental conditions shown in *D* (vehicle $n = 21$ cells from 6 mice; CT-99021 $n = 27$ cells from 8 mice; triciribine $n = 24$ cells from 7 mice; AAV-shCTRL $n = 26$ cells from 7 mice; AAV-shGSK3β $n = 25$ cells from 7 mice).

significant increase of A-type K^+ current density was found compared with the current density measured in AAV-shCTRL-transfected neurons (AAV-shGSK3β-GFP: 17.0 ± 1.7 pA/pF, $n = 25$; AAV-shCTRL-GFP: 11.1 ± 1.8 pA/pF; $n = 26$; unpaired Student's *t*-test $P < 0.05$). These results further support our contention that GSK3β regulates tLTD via modulation of Kv4.2 channels.

GSK3β–KV4.2 Interaction

To characterize the interaction of GSK3β and Kv4.2 in layer 2/3 pyramidal neurons of somatosensory cortex we first asked whether GSK3β and Kv4.2 proteins colocalize in this brain area. High-resolution confocal microscope images showed overlapping immunofluorescence signals of GSK3β and Kv4.2 in both soma and dendrites (colocalization indices: Rr = 0.4 ± 0.016; R = 0.67 ± 0.02), suggesting a possible physical interaction of the 2 proteins (Fig. 5A,B).

To test this hypothesis coimmunoprecipitation experiments were performed with total somatosensory cortex lysates. This assay revealed that using an anti-GSK3β antibody the Kv4.2 channel coimmunoprecipitated (Co-IP) with GSK3β (Fig. 5C). Together, these results demonstrate that GSK3β and Kv4.2 physically interact in somatosensory cortex.

A number of studies have demonstrated complex phosphorylation-dependent regulation of Kv4.2 α-subunit with functional consequences on transient A-type K^+ currents. In vitro phosphorylation of recombinant fragments of Kv4.2 revealed PKA- (Anderson et al. 2000), ERK- (Adams et al. 2000), and CaMKII- (Varga et al. 2004) mediated phosphorylation of Kv4.2 channel. More recently, we showed that treatment of hippocampal neurons with amyloid-β protein ($A\beta_{42}$) induces a decrease of A-type K^+ currents and an increase in excitability through a GSK3-dependent mechanism. Interestingly, these effects were paralleled with phosphorylation of Kv4.2 at Ser-616 (Scala et al. 2015). Although this study suggested that Ser-616 of Kv4.2 subunit might be a phosphorylation target for GSK3 leading to functional outcomes for K^+ currents, the demonstration of whether GSK3β indeed phosphorylates Ser-616 site and whether this occurs in a direct or indirect way is still missing. Thus, in order to gain further insight into the phosphorylation-dependent regulation of Kv4.2 channel by GSK3β, we first overexpressed Kv4.2 channel-EGFP in human embryonic kidney (HEK) 293 cell line and confirmed the association of the exogenously expressed Kv4.2 protein with GSK3β by Co-IP (Supplementary Fig. S5A). Control cells were transfected with a EGFP-empty vector. We then preincubated HEK293 cells expressing Kv4.2 subunit with CT-99021 (3 μM; 60 min) and triciribine (10 μM; 60 min) and performed Western blot analysis of total cell lysates to examine the phosphorylation levels of Ser-616. As shown in Figure 6, CT-99021 treatment led to a significant decrease ($P < 0.05$; $n = 3$) in Ser-616 phosphorylation compared with vehicle (DMSO). On the contrary, triciribine had an opposite effect, increasing the Ser-616 phosphorylation level ($P < 0.05$; $n = 3$). Importantly, when HEK293 cells were transfected with a mutant form of Kv4.2, bearing a serine to alanine substitution at residue 616 ($Kv4.2^{S616A}$), Ser-616 phosphorylation was completely absent in

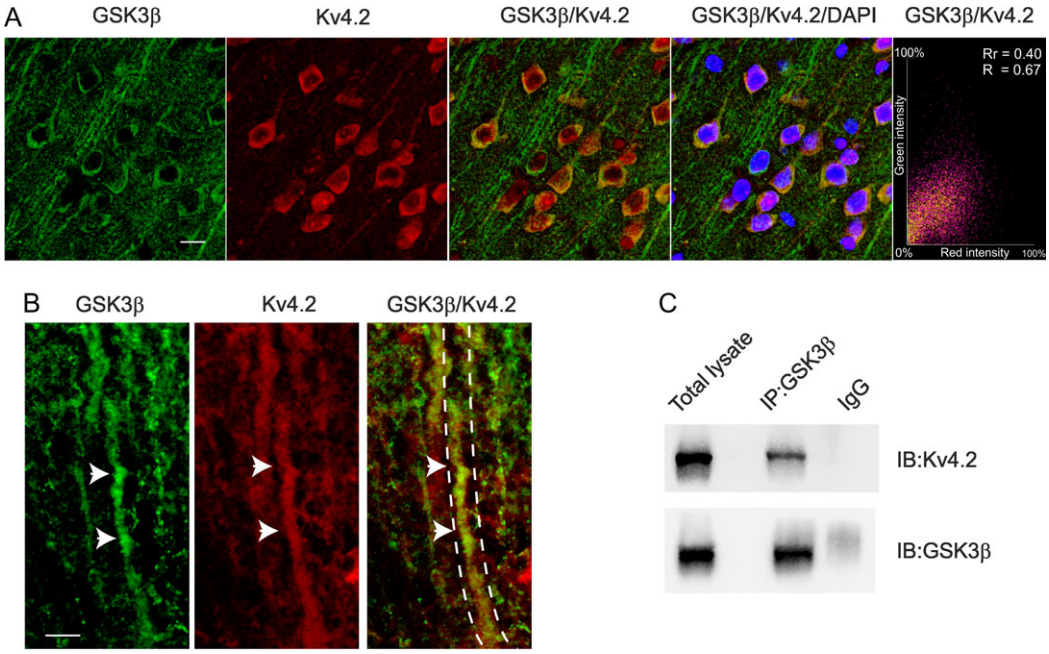

Figure 5. Kv4.2 and GSK3β proteins colocalize and physically interact into somatosensory cortex. (*A*) GSK3β (green) and Kv4.2 (red) were both expressed in the cell soma and dendrites (scale bar 25 μm). The last right panel shows the red–green correlation plot for GSK3β and Kv4.2 colocalization, both Pearson's correlation (Rr) and Manders' Overlap coefficient (*R*) are shown. Nuclei were counterstained with DAPI. (*B*) High coexpression of the 2 proteins in the dendrites is also shown (arrows) in the higher magnification (single and merged) images (scale bar 5 μm). (*C*) Coimmunoprecipitation experiment between GSK3β and Kv4.2. Lysate of somatosensory cortex was immunoprecipitated (IP) with an antibody against GSK3β or with rabbit immunoglobulins (IgG, as control) and the membrane was immunoblotted with anti-GSK3β or Kv4.2. The antibody against GSK3β, but not the rabbit IgG, precipitated a band corresponding to Kv4.2.

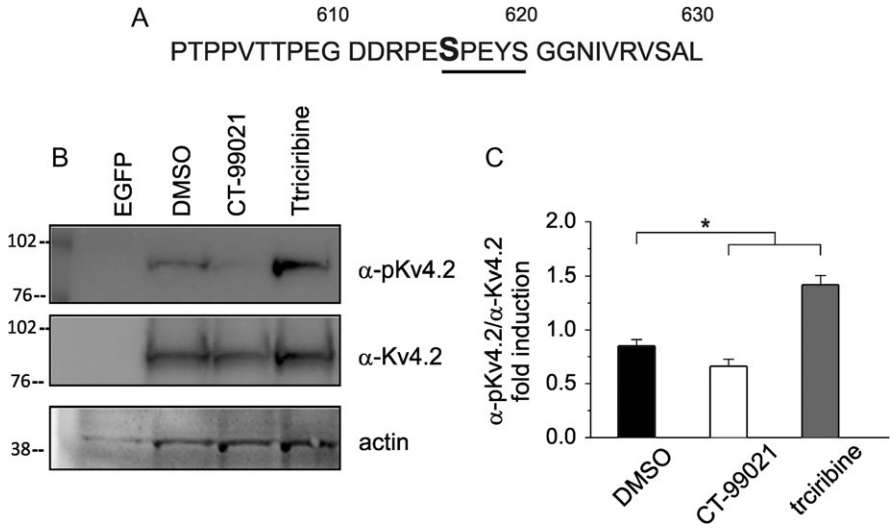

Figure 6. Phosphorylation of Kv4.2 at Ser-616 is inversely modulated by CT-99021 and triciribine. (*A*) Primary sequence of the C-terminal domain of Kv4.2 channel around the putative GSK3β phosphorylation site Ser-616. (*B*) Representative blots of total cell lysate from HEK293 transfected for 48 h with Kv4.2-WT plasmid or empty vector (EGFP) probed with either anti-phospho-Ser-616 or total Kv4.2 antibodies following treatment with CT99021 (3 μM, 1 h), triciribine (10 μM, 1 h) or vehicle (DMSO). (*C*) Densitometric analysis for the blots probed with the anti-phospho-Ser-616 (α-pKv4.2) and normalized to total Kv4.2 (α-Kv4.2) channel is shown ($n = 3$; $P < 0.05$; statistics by Mann–Whitney test).

all experimental conditions (Supplementary Fig. S5C). These results indicate that Ser-616 of Kv4.2 subunit is indeed a direct downstream target of GSK3β.

We next performed whole-cell patch-clamp recordings on HEK293 cells transfected with Kv4.2 subunit and compared the magnitude of the pure Kv4.2-mediated K^+ currents during intracellular perfusion of CT-99021, triciribine and vehicle in voltage-clamp mode. As shown in Supplementary Figure S6, Kv4.2 channel currents exhibited rapid activation and inactivation that are typical of A-type K^+ currents.

After 10 min (T_{10}) of CT-99021 perfusion the Kv4.2 currents significantly increased compared with those recorded right after achieving whole-cell configuration (T_0) (Fig. 7A,B,E,F; normalized K^+ current at T_0 was 1.00 ± 0.01 vs. 1.31 ± 0.01 at T_{10};

$n = 10$; $P < 0.001$; paired t-test). The CT-99021-induced current enhancement developed quite slowly and peaked ~10 min after intracellular application of CT-99021 (Fig. 7E). To rule out non-specific effects of CT-99021, K^+ currents were examined after cells injection with vehicle. As shown in Figure 7E,F, vehicle did not significantly affect K^+ currents (normalized K^+ current at T_0 was 1.0 ± 0.01 vs. 0.95 ± 0.3 at T_{10}; $n = 10$; $P > 0.05$; paired t-test). On the contrary, by enhancing the pool of active GSK3β through triciribine-mediated Akt-1 inhibition, a significant decrease of A-type K^+ currents, with a time course similar to CT-99021-induced effect, was found (Fig. 7C,D, E,F; normalized K^+ current at T_0 was 0.99 ± 0.01 vs. 0.72 ± 0.01 at T_{10}; $n = 12$; $P < 0.001$; paired t-test). Interestingly, when HEK293 cells were transfected with the mutant $Kv4.2^{S616A}$, no changes of Kv4.2 potassium currents were detected during 10-min intracellular perfusion of either CT-99021 or triciribine (Fig. 7G; CT-99021: normalized K^+ current at $T_0 = 0.99 \pm 0.01$, normalized K^+ current at $T_{10} = 0.97 \pm 0.01$, $n = 10$, $P > 0.05$, paired t-test; triciribine: normalized K^+ current at $T_0 = 0.98 \pm 0.01$, normalized K^+ current at $T_{10} = 0.97 \pm 0.01$, $n = 10$; $P > 0.05$; paired t-test). These results strongly indicate that GSK3β-mediated direct phosphorylation of Ser-616 decreases Kv4.2 activity.

Collectively, our results identify a novel functional interaction of GSK3β with the Kv4.2 channel as a novel mechanism for tLTD modulation.

Discussion

Here we report a novel mechanism by which GSK3β regulation of Kv4.2 channels in layer 2/3 pyramidal neurons of somatosensory cortex modulates tLTD. Four experimental evidences support this conclusion: (1) pharmacological agents affecting the levels of active GSK3 and GSK3β knockdown result in tLTD and A-type K^+ current modulation; (2) the pharmacological blockade of A-type K^+ current occludes the triciribine-induced effect on tLTD; (3) Kv4.2 coimmunoprecipitates and colocalizes with GSK3β; and (4) in HEK293 cells expressing Kv4.2 channels GSK3β-mediated direct phosphorylation of the consensus site Ser-616 of Kv4.2 decreases channel activity.

GSK3β is a kinase that has been long recognized as a critical effector in the cell and an important target for therapeutic interventions based on its involvement in many diseases (Jope 2011; Giese 2009; Kremer et al. 2011). Only recently, however, it has been unveiled that GSK3β is also a key regulator of synaptic plasticity. The first observation demonstrating a role for GSK3β in synaptic plasticity was reported by Collingridge's group (Peineau et al. 2008). This seminal study showed that GSK3β activity is required for the induction of NMDA-dependent LTD in hippocampus. Moreover, these authors showed that the induction of LTP inhibits LTD via regulation of GSK3β, NMDA receptors and PI3-Akt pathway. Following this study a number of investigations have been conducted focusing on: (1) the downstream effectors of GSK3β in synaptic plasticity; (2) the upstream regulation of GSK3β in synaptic plasticity; (3) the role of GSK3β in pathological synaptic plasticity; and (4) the role in synaptic plasticity at GABAergic synapses. Within this context, our demonstration that GSK3β modulates STDP in somatosensory cortex provides novel evidence for the involvement of GSK3β in synaptic plasticity.

Our demonstration that bidirectional modulation of GSK3 affect tLTD is based on electrophysiological data showing marked increase in tLTD when layer 2/3 pyramidal neurons were intracellularly perfused with the GSK3 inhibitor, CT-99021. Furthermore, this finding was strongly corroborated by the fact that GSK3β knockdown results in a similar effect on tLTD amplitude. Conversely, inhibition of Akt1, a kinase inhibiting GSK3, by its selective inhibitor triciribine lead to an opposite modulation of tLTD. It should be pointed out that these pharmacological agents have been widely used to demonstrate the GSK3 role in synaptic plasticity and other functions (Jo et al. 2011; Yue et al. 2017; Forkwa et al. 2014). In particular, CT-99021 is a potent and highly selective inhibitor of GSK3 (IC50 values are 6.7 and 10 nM for GSK3β and GSK3α, respectively). An in vitro study has demonstrated that CT-99021 was the most potent and specific among different GSK3 inhibitors, that is, CT-99021, AR-A0-144-18, SB 216 763, SB 415 286, alsterpaullone, kenpaullone, and LiCl (Bain et al. 2007). It inhibited Cyclin-dependent kinase (CDK2), its closest homologs kinase, about 50-fold less potently and did not affect many other protein kinases at 1 μM concentration (Bain et al. 2007). Moreover, 1–2 μM CT-99021 has been previously used in electrophysiological experiments by different authors (Jo et al. 2011; Chen et al. 2015; Franklin et al. 2014; Kailainathan et al. 2016).

With regard to the selectivity of triciribine on Akt signaling pathways (also known as AKT/protein kinase B signaling inhibitor-2), it is noteworthy that this compound inhibits the phosphorylation, activation and signaling of Akt without any inhibitory effects on a number of others kinases examined (Yang et al. 2004). We used 10 μM triciribine in accordance with previous reports (Yang et al. 2004; Forkwa et al. 2014; Gómez-Hurtado et al. 2014; Yue et al. 2017).

With regard to the GSK3 isoforms involved in tLTD regulation, our results obtained in mice with GSK3β silencing strongly support a prominent role for this isoform though a complementary role for GSK3α cannot be excluded.

It is well known that A-type K^+ channels contribute to the regulation of synaptic strength in hippocampus and other brain regions (Kim and Hoffman 2008; Labno et al. 2014; Yang et al. 2014). The rapidly activating and inactivating voltage-gated A-type K^+ current is broadly expressed in neurons and is a key regulator of AP repolarization, repetitive firing, back propagation of action potentials, and responses to synaptic inputs (Cai et al. 2004; Yuan et al. 2005; Norris and Nerbonne 2010). In the brain A-type currents can be generated by Kv1.4, Kv3.4, and any of the Kv4 family subunits (Kv4.1, Kv4.2, and Kv4.3) and a large body of evidence indicates that Kv4 channels are localized particularly in dendrites and the soma of many types of neurons, including hippocampal and cortical neurons (Rhodes et al. 2004). Blocking A-type K^+ currents in dendrites with 4-aminopyridine enhances the back propagation of dendritic APs and boosts EPSPs (Hoffman et al. 1997). Furthermore, the gating property and distribution of A-type K^+ channels influence the intracellular Ca^{2+} levels in dendritic branches, as demonstrated by changes in dendritic Ca^{2+} influx during AP back-propagation by genetic down or up-regulation of Kv4.2 (Chen et al. 2006). Because Ca^{2+} influx through NMDA receptors is fundamental for many forms of synaptic plasticity in dendrites, the regulatory effects of A-type K^+ channels (i.e., Kv4.2) on dendritic excitability are consequential critical for dendritic and synaptic processing during synaptic plasticity. Indeed, the requirement of the modulatory function of A-type K^+ channels has been demonstrated by different studies using stimulating protocols that rely on AP back-propagation for LTP induction (Ramakers and Storm 2002; Chen et al. 2006; Jung et al. 2008). These studies have also demonstrated that the LTP threshold is reduced by down regulation of A-type K^+ channels. The involvement of Kv4.2 channels modulation in mediating the GSK3β effects on tLTD is fully supported by our data demonstrating

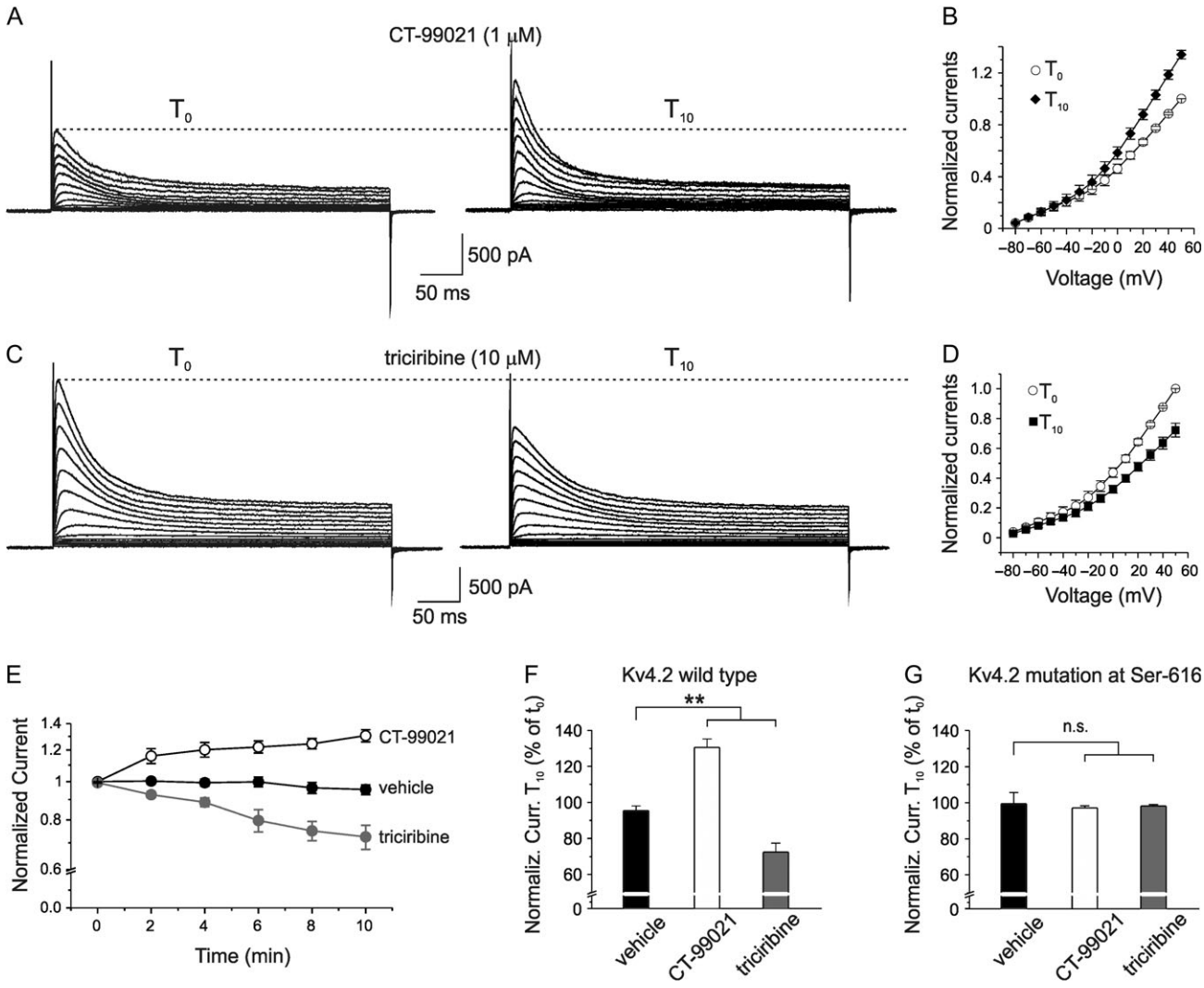

Figure 7. Intracellular perfusion of GSK3 modulators affect Kv4.2-induced A-type K^+ currents in HEK293 cells. (*A*) Whole-cell recordings from a HEK293 cell expressing Kv4.2 subunit in voltage-clamp configuration showing an increase in K^+ currents after 10 min of intracellular perfusion of GSK3 blocker CT-99021 (1 μM) via the patch-pipette. (*B*) Mean normalized *I-V* relationship of the CT-99021 effect ($n = 10$). (*C*) Representative traces shoving that intracellular triciribine perfusion decreased K^+ currents. (*D*) Mean normalized I-V relationship of the experiment showed in *C* ($n = 12$). (*E*) Time course of the normalized Kv4.2-induced K^+ current during intracellular perfusion of CT-99021 ($n = 10$), triciribine ($n = 12$), and vehicle ($n = 10$) that had no effects on K^+ currents. (*F*) Bar graph summarizing data from experiments shown in *E* and performed on HEK293 cell expressing wild type Kv4.2 subunit. Multiple comparisons were performed with ANOVA test with Tukey post hoc ($F_{(2,28)} = 51.3$; $P < 0.001$). Data are expressed as percentage of the peak K^+ current at +50 mV recorded after 10 min of intracellular perfusion of CT-99021, triciribine and vehicle (T_{10}) versus that recorded soon after establishing the whole-cell configuration (T_0). (*G*) Bar graph summarizing data from experiments in which HEK293 cells were transfected with the mutant $Kv4.2^{S616A}$ (ANOVA test with Tukey post hoc $F_{(2,28)} = 0.12$; $P > 0.5$).

that pharmacological blockade of these channels by 4-AP and AmmTX3 mimics and occludes the triciribine's effect on tLTD. Moreover, our results exclude the involvement of Kv1 channels in GSK3β-dependent modulation of tLTD. This is in accordance with previous observations reporting that APs are only partially repolarized by these channels in pyramidal neurons of the mouse neocortex (Pathak et al. 2016). In addition, we show that pharmacological agents affecting the levels of active GSK3 and GSK3β knockdown by sh-interference result in A-type K^+ current modulation.

A proposed cellular mechanism for STDP postulates that the magnitude of NMDAR-dependent calcium signal (along with calcium entering through VGCCs) determines the sign of plasticity. With regard to tLTD, it has been shown that pairing protocol (post-leading-pre) generates weak calcium signal at postsynaptic level because EPSP coincides with the modest afterdepolarization following bAP, thus generating NMDA currents only modestly greater than those occurring at resting membrane potential (Feldman 2012; Karmarkar and Buonomano 2002; Shouval et al. 2002; Nevian and Sakmann 2006). We speculate that in experimental conditions in which GSK3β is downregulated (i.e., CT-99021 or AAV-shGSK3β-GFP) the subsequent increase in A-type K^+ current leads to a reduced dendritic Ca^{2+} influx during AP back-propagation and, as a consequence, increased tLTD amplitude. On the contrary, upregulation of GSK3β and subsequent reduction of A-type K^+ conductance leads to a facilitation of dendritic AP propagation and, therefore, reduced tLTD by increased dendritic Ca^{2+} influx.

Our immunohistochemical results clearly demonstrate colocalization between immunoreactivity for GSK3β and for Kv4.2 in soma and dendrites of layer 2/3 somatosensory cortex. This cellular colocalization, which is consistent with results

reported in previous studies using single immunoreactivity in neocortex (Rhodes et al. 2004; Lee et al. 2006), together with our coimmunoprecipitation results strongly strengthen the notion that GSK3β and Kv4.2 may form a molecular and functional complex in the somatosensory cortex.

How might GSK3β modulate Kv4.2 activity? In a recent study we discovered that treatment of hippocampal neurons with $A\beta_{42}$ results in GSK-3-dependent Kv4.2 phosphorylation at Ser-616 (Scala et al. 2015). Therefore, the evidence that Kv4.2 is a putative GSK-3 target was already suggested. In this study we confirm this finding and show that the ability of GSK3β to phosphorylate Kv4.2 subunits is mediated by a direct mechanism. Indeed, our results indicate that in HEK293 cells expressing only Kv4.2 subunits the modulation of active GSK3β levels strongly affects the phosphorylation of Kv4.2 at Ser-616. Furthermore, we show that the outcome of GSK3β-mediated direct phosphorylation of Kv4.2 α-subunit is a decreased channel activity in accordance to our electrophysiological experiments performed in layer 2/3 pyramidal neurons. These findings are in agreement with previous studies demonstrating complex phosphorylation-dependent regulation of Kv4.2 with functional consequences on transient A-type K^+ currents. In this regard, it should be noted that in vitro phosphorylation of recombinant fragments of Kv4.2 revealed CaMKII- (Varga et al. 2004) PKA- (Anderson et al. 2000) and ERK- (Adams et al. 2000) mediated phosphorylation of Kv4.2. It is noteworthy that ERK-mediated phosphorylation of Kv4.2 leads to decreased Kv4.2 current and that ERK directly phosphorylates Kv4.2 at Ser-616 (Schrader et al. 2006). The consensus sequence for GSK-3 targets typically consists of S/T-X-X-X-S/T in which the first S/T residue is the GSK-3 phosphorylation site (Jope and Johnson 2004; Wildburger and Laezza 2012). Importantly, Ser-616 of Kv4.2 resides within a putative GSK3β consensus motif.

With regard to the possible correlations between our findings and others tLTD modulatory mechanisms it should be considered that in many brain regions, including neocortex, tLTD requires activity-dependent postsynaptic release of an endocannabinoid (eCB) (Sjöström et al. 2003; Feldman 2012; Banerjee et al. 2016). In particular, the proposed model for endocannabinoids-dependent tLTD suggests that during timing-dependent LTD induction, presynaptically released glutamate activates mGluRs and postsynaptic APs enhance Ca^{2+} influx through VGCCs, leading to synthesis of eCBs which diffuse in a retrograde manner and bind to presynaptic and/or astrocytic CB1 receptors. Coactivation of presynaptic CB1 receptors (CB1Rs) and presynaptic NMDA receptors causes synaptic depression. Alternatively, activation of astrocytic CB1Rs results in astrocytic release of glutamate or D-serine, which activates presynaptic NMDARs (Sjöström et al. 2003; Bender et al. 2006; Nevian and Sakmann 2006; Min and Nevian 2012; Banerjee et al. 2016). A recent work showed that 2-arachidonoyl glycerol (2-AG), the major endocannabinoid in the mammalian brain, besides activation of cannabinoids receptors, can directly alter the properties of A-type K^+ channels and accelerate the pacemaker activity of rodent dopamine neurons (Gantz and Bean 2017). In particular, this study demonstrates that activation of Gq-coupled receptors expressed on dopaminergic neurons, triggers 2-AG synthesis through phospholipase C (PLC) activation, and 2-AG-dependent inhibition of A-type K^+ channels leading to increased neuronal excitability. These findings, together with the notion that A-type K^+ channel modulation affects STDP (Chen et al. 2006; Jung et al. 2008) allows to hypothesize that eCBs may affect tLTD also through a postsynaptic mechanism. Moreover, since CBs can directly modulate Akt/GSK3β pathway in different brain regions, including the neocortex (Ozaita et al. 2007) it is also tempting to speculate a possible correlation between GSK3β-dependent modulation of tLTD and cannabinoid signaling pathway.

With regard to the potential implications of our findings on cortical functions it is noteworthy to recall that synapses in the layer 2/3 of primary somatosensory cortex provide a good model to study synaptic mechanisms of receptive field plasticity (Feldman and Brecht 2005; Petersen and Crochet 2013). Somatosensory maps are highly plastic, both during development (Simons and Land 1987) and in adult animals (Buonomano and Merzenich 1998). Plasticity occurs in response to train on sensory tasks, passive sensory experience and peripheral lesions. Therefore, the underlying cellular mechanisms for map plasticity are highly relevant to learning, development and recovery after brain injury. The GSK3β/Kv4.2-mediated modulation of tLTD we observed in this study represent one additional cellular/synaptic modulatory mechanism by which plasticity occurs in somatosensory cortex.

In conclusion, our data provide the first evidence linking GSK3β and Kv4.2 channels function with tLTD modulation in the somatosensory cortex and propose a model that may be relevant for studying the physiology associated with cortical map plasticity and development.

Authors' Contributions

G.A. designed, performed and analyzed electrophysiological experiments; A.R. performed Western blot experiments; A.M. and S.F. performed co-IP experiments; C.C., S.A.B. and G.A., performed immunohistochemical experiments; L.L., K.G. and G.A. performed single cell reverse transcription quantitative real-time PCR; M.R. performed viral injection; F.L., F.S. and T.G. contributed to design experiments and to review the article; M.D. and C.G. conceived the study supervised the work and wrote the article. All authors gave approval to the final version of the article.

Supplementary Material

Supplementary material is available at *Cerebral Cortex* online.

Funding

Grant from Università Cattolica (D1-2017, #4124500559 to C.G.), (DA029091 to T.A.G.), (NS081121 to T.A.G.), (MH107609 to F.L.), (MH095995 to F.L.) and John Sealy Memorial Endowment Funds (F.L.) from the University of Texas Medical Branch.

Notes

Conflict of Interest: None declared.

References

Adams JP, Anderson AE, Varga AW, Dineley KT, Cook RG, Pfaffinger PJ, Sweatt JD. 2000. The A-type potassium channel Kv4.2 is a substrate for the mitogen-activated protein kinase ERK. J Neurochem. 75:2277–2287.

Agmon A, Connors BW. 1991. Thalamocortical responses of mouse somatosensory (barrel) cortex in vitro. Neuroscience. 41:365–379.

Agmon A, Connors BW. 1992. Correlation between intrinsic firing patterns and thalamocortical synaptic responses of neurons in mouse barrel cortex. J Neurosci. 12:319–329.

Ali A, Hoeflich KP, Woodgett JR. 2001. Glycogen synthase kinase-3: properties, functions, and regulation. Chem Rev. 101:2527–2540.

Anderson AE, Adams JP, Qian Y, Cook RG, Pfaffinger PJ, Sweet JD. 2000. Kv4.2 phosphorylation by cyclic AMP-dependent protein kinase. J Biol Chem. 275:5337–5346.

Bain J, Plater L, Elliott M, Shpiro N, Hastie CJ, McLauchlan H, Klevernic I, Arthur JS, Alessi DR, Cohen P. 2007. The selectivity of protein kinase inhibitors: a further update. Biochem J. 408:297–315.

Banerjee A, González-Rueda A, Sampaio-Baptista C, Paulsen O, Rodríguez-Moreno A. 2014. Distinct mechanisms of spike timing-dependent LTD at vertical and horizontal inputs onto L2/3 pyramidal neurons in mouse barrel cortex. Physiol Rep. 2:e00271.

Banerjee A, Larsen RS, Philpot BD, Paulsen O. 2016. Roles of presynaptic NMDA receptors in neurotransmission and plasticity. Trends Neurosci. 39:26–39.

Banerjee A, Meredith RM, Rodríguez-Moreno A, Mierau SB, Auberson YP, Paulsen O. 2009. Double dissociation of spike timing-dependent potentiation and depression by subunit-preferring NMDA receptor antagonists in mouse barrel cortex. Cereb Cortex. 19:2959–2969.

Bender VA, Bender KJ, Brasier DJ, Feldman DE. 2006. Two coincidence detectors for spike timing-dependent plasticity in somatosensory cortex. J Neurosci. 26:4166–4177.

Benzon CR, Johnson SB, McCue DL, Li D, Green TA, Hommel JD. 2014. Neuromedin U receptor 2 knockdown in the paraventricular nucleus modifies behavioral responses to obesogenic high-fat food and leads to increased body weight. Neuroscience. 258:270–279.

Beurel E, Grieco SF, Jope RS. 2015. Glycogen synthase kinase-3 (GSK3): regulation, actions, and diseases. Pharmacol Ther. 148:114–131.

Bouvier G, Bidoret C, Casado M, Paoletti P. 2015. Presynaptic NMDA receptors: roles and rules. Neuroscience. 311:322–340.

Bovetti S, Moretti C, Zucca S, Dal Maschio M, Bonifazi P, Fellin T. 2017. Corrigendum: simultaneous high-speed imaging and optogenetic inhibition in the intact mouse brain. Sci Rep. 7:46122.

Boyle WJ, Smeal T, Defize LH, Angel P, Woodgett JR, Karin M, Hunter T. 1991. Activation of protein kinase C decreases phosphorylation of c-Jun at sites that negatively regulate its DNA-binding activity. Cell. 64:573–584.

Bradley CA, Peineau S, Taghibiglou C, Nicolas CS, Whitcomb DJ, Bortolotto ZA, Kaang BK, Cho K, Wang YT, Collingridge GL. 2012. A pivotal role of GSK-3 in synaptic plasticity. Front Mol Neurosci. 15:5–13.

Buonomano DV, Merzenich MM. 1998. Net interaction between different forms of short-term synaptic plasticity and slow-IPSPs in the hippocampus and auditory cortex. J Neurophysiol. 80:1765–1774.

Cadwell CR, Palasantza A, Jiang X, Berens P, Deng Q, Yilmaz M, Reimer J, Shen S, Bethge M, Tolias KF, et al. 2016. Electrophysiological, transcriptomic and morphologic profiling of single neurons using Patch-seq. Nat Biotechnol. 34:199–203.

Cai X, Liang CW, Muralidharan S, Kao JP, Tang CM, Thompson SM. 2004. Unique roles of SK and Kv4.2 potassium channels in dendritic integration. Neuron. 44:351–364.

Carter BC, Jahr CE. 2016. Postsynaptic, not presynaptic NMDA receptors are required for spike-timing-dependent LTD induction. Nat Neurosci. 19:1218–1224.

Chen X, Yuan LL, Zhao C, Birnbaum SG, Frick A, Jung WE, Schwarz TL, Sweatt JD, Johnston D. 2006. Deletion of Kv4.2 gene eliminates dendritic A-type K+ current and enhances induction of long-term potentiation in hippocampal CA1 pyramidal neurons. J Neurosci. 26:12143–12151.

Chen RJ, Zhang G, Garfield SH, Shi YJ, Chen KG, Robey PG, Leapman RD. 2015. Variations in glycogen synthesis in human pluripotent stem cells with altered pluripotent states. PLoS One. 10:e0142554.

Connors BW, Gutnick MJ. 1990. Intrinsic firing patterns of diverse neocortical neurons. Trends Neurosci. 13:99–104.

Corlew R, Wang Y, Ghermazien H, Erisir A, Philpot BD. 2007. Developmental switch in the contribution of presynaptic and postsynaptic NMDA receptors to long-term depression. J Neurosci. 27:9835–9845.

Crofton EJ, Nenov MN, Zhang Y, Scala F, Page SA, McCue DL, Li D, Hommel JD, Laezza F, Green TA. 2017. Glycogen synthase kinase 3 beta alters anxiety-, depression-, and addiction-related behaviors and neuronal activity in the nucleus accumbens shell. Neuropharmacology. 117:49–60.

Cross DA, Alessi DR, Cohen P, Andjelkovich M, Hemmings BA. 1995. Inhibition of glycogen synthase kinase-3 by insulin mediated by protein kinase B. Nature. 378:785–789.

Doble BW, Woodgett JR. 2003. GSK-3: tricks of the trade for a multi-tasking kinase. J Cell Sci. 116:1175–1186.

Duan KZ, Xu Q, Zhang XM, Zhao ZQ, Mei YA, Zhang YQ. 2012. Targeting A-type K(+) channels in primary sensory neurons for bone cancer pain in a rat model. Pain. 153:562–574.

Emamian ES. 2012. AKT/GSK3 signaling pathway and schizophrenia. Front Mol Neurosci. 15:5–33.

Emamian ES, Hall D, Birnbaum MJ, Karayiorgou M, Gogos JA. 2004. Convergent evidence for impaired AKT1-GSK3beta signaling in schizophrenia. Nat Genet. 36:131–137.

Fang X, Yu SX, Lu Y, Bast RC Jr, Woodgett JR, Mills GB. 2000. Phosphorylation and inactivation of glycogen synthase kinase 3 by protein kinase A. Proc Natl Acad Sci U S A. 97:11960–11965.

Feldman DE. 2000. Timing-based LTP and LTD at vertical inputs to layer II/III pyramidal cells in rat barrel cortex. Neuron. 27:45–56.

Feldman DE. 2012. The spike-timing dependence of plasticity. Neuron. 75:556–571.

Feldman DE, Brecht M. 2005. Map plasticity in somatosensory cortex. Science. 310:810–815.

Forkwa TK, Neumann ID, Tamm ER, Ohlmann A, Reber SO. 2014. Short-term psychosocial stress protects photoreceptors from damage via corticosterone-mediated activation of the AKT pathway. Exp Neurol. 252:28–36.

Frame S, Cohen P. 2001. GSK3 takes centre stage more than 20 years after its discovery. Biochem J. 359:1–16.

Franklin AV, King MK, Palomo V, Martinez A, McMahon LL, Jope RS. 2014. Glycogen synthase kinase-3 inhibitors reverse deficits in long-term potentiation and cognition in fragile X mice. Biol Psychiatry. 75:198–206.

Froemke RC. 2015. Plasticity of cortical excitatory-inhibitory balance. Annu Rev Neurosci. 38:195–219.

Gantz SC, Bean BP. 2017. Cell-autonomous excitation of midbrain dopamine neurons by endocannabinoid-dependent lipid signaling. Neuron. 93:1375–1387.e2.

Giese KP. 2009. GSK-3: a key player in neurodegeneration and memory. IUBMB Life. 61:516–521.

Goode N, Hughes K, Woodgett JR, Parker PJ. 1992. Differential regulation of glycogen synthase kinase-3 beta by protein kinase C isotypes. J Biol Chem. 267:16878–16882.

Grimes CA, Jope RS. 2001. The multifaceted roles of glycogen synthase kinase 3beta in cellular signaling. Prog Neurobiol. 65:391–426.

Gómez-Hurtado N, Fernández-Velasco M, Fernández-Alfonso MS, Boscá L, Delgado C. 2014. Prolonged leptin treatment increases transient outward K^+ current via upregulation of Kv4.2 and Kv4.3 channel subunits in adult rat ventricular myocytes. Pflugers Arch. 466:903–914.

Hoffman DA, Johnston D. 1998. Downregulation of transient K^+ channels in dendrites of hippocampal CA1 pyramidal neurons by activation of PKA and PKC. J Neurosci. 18:3521–3528.

Hoffman DA, Magee JC, Colbert CM, Johnston D. 1997. K+ channel regulation of signal propagation in dendrites of hippocampal pyramidal neurons. Nature. 387:869–875.

Hooper C, Killick R, Lovestone S. 2008. The GSK3 hypothesis of Alzheimer's disease. J Neurochem. 104:1433–1439.

House DR, Elstrott J, Koh E, Chung J, Feldman DE. 2011. Parallel regulation of feedforward inhibition and excitation during whisker map plasticity. Neuron. 72:819–831.

Hsu WC, Nenov MN, Shavkunov A, Panova N, Zhan M, Laezza F. 2015. Identifying a kinase network regulating FGF14:Nav1.6 complex assembly using split-luciferase complementation. PLoS One. 10:e0117246.

Jiang X, Shen S, Cadwell CR, Berens P, Sinz F, Ecker AS, Patel S, Tolias AS. 2015. Principles of connectivity among morphologically defined cell types in adult neocortex. Science. 350: aac9462.

Jiang N, Shi P, Desland F, Kitchen-Pareja MC, Sumners C. 2013. Interleukin-10 inhibits angiotensin II-induced decrease in neuronal potassium current. Am J Physiol Cell Physiol. 304: C801–C807.

Jo J, Whitcomb DJ, Olsen KM, Kerrigan TL, Lo SC, Bru-Mercier G, Dickinson B, Scullion S, Sheng M, Collingridge G, et al. 2011. Aβ(1–42) inhibition of LTP is mediated by a signaling pathway involving caspase-3, Akt1 and GSK-3β. Nat Neurosci. 14: 545–547.

Jope RS. 2011. Glycogen synthase kinase-3 in the etiology and treatment of mood disorders. Front Mol Neurosci. 9:4–16.

Jope RS, Johnson GV. 2004. The glamour and gloom of glycogen synthase kinase-3. Trends Biochem Sci. 29:95–102.

Jung SC, Kim J, Hoffman DA. 2008. Rapid, bidirectional remodeling of synaptic NMDA receptor subunit composition by A-type K+ channel activity in hippocampal CA1 pyramidal neurons. Neuron. 60:657–671.

Kaidanovich-Beilin O, Woodgett JR. 2011. GSK-3: functional insights from cell biology and animal models. Front Mol Neurosci. 16:4–40.

Kailainathan S, Piers TM, Yi JH, Choi S, Fahey MS, Borger E, Gunn-Moore FJ, O'Neill L, Lever M, Whitcomb DJ, et al. 2016. Activation of a synapse weakening pathway by human Val66 but not Met66 pro-brain-derived neurotrophic factor (proBDNF). Pharmacol Res. 104:97–107.

Karmarkar UR, Buonomano DV. 2002. A model of spike-timing dependent plasticity: one or two coincidence detectors? J Neurophysiol. 88:507–513.

Kim J, Hoffman DA. 2008. Potassium channels: newly found players in synaptic plasticity. Neuroscientist. 14:276–286.

Kockeritz L, Doble B, Patel S, Woodgett JR. 2006. Glycogen synthase kinase-3-an overview of an over-achieving protein kinase. Curr Drug Targets. 7:1377–1388.

Kremer A, Louis JV, Jaworski T, Van Leuven F. 2011. GSK3 and Alzheimer's disease: facts and fiction. Front Mol Neurosci. 26:4–17.

Labno A, Warrier A, Wang S, Zhang X. 2014. Local plasticity of dendritic excitability can be autonomous of synaptic plasticity and regulated by activity-based phosphorylation of Kv4.2. PLoS One. 9:e84086.

Lee SJ, Chung YH, Joo KM, Lim HC, Jeon GS, Kim D, Lee WB, Kim YS, Cha CI. 2006. Age-related changes in glycogen synthase kinase 3beta (GSK3beta) immunoreactivity in the central nervous system of rats. Neurosci Lett. 409:134–139.

Li Q, Fleming RL, Acheson SK, Madison RD, Moore SD, Risher ML, Wilson WA, Swartzwelder HS. 2013. Long-term modulation of A-type K(+) conductances in hippocampal CA1 interneurons in rats after chronic intermittent ethanol exposure during adolescence or adulthood. Alcohol Clin Exp Res. 37: 2074–2085.

Li M, Wang X, Meintzer MK, Laessig T, Birnbaum MJ, Heidenreich KA. 2000. Cyclic AMP promotes neuronal survival by phosphorylation of glycogen synthase kinase 3beta. Mol Cell Biol. 20:9356–9363.

Lovestone S, Killick R, Di Forti M, Murray R. 2007. Schizophrenia as a GSK-3 dysregulation disorder. Trends Neurosci. 30:142–149.

Lucas FR, Goold RG, Gordon-Weeks PR, Salinas PC. 1998. Inhibition of GSK-3β leading to the loss of phosphorylated MAP-1B is an early event in axonal remodelling induced by WNT-7a or lithium. J Cell Sci. 111:1351–1361.

Maffie JK, Dvoretskova E, Bougis PE, Martin-Eauclaire MF, Rudy B. 2013. Dipeptidyl-peptidase-like-proteins confer high sensitivity to the scorpion toxin AmmTX3 to Kv4-mediated A-type K+ channels. J Physiol. 591:2419–2427.

Meitzen J, Weaver AL, Brenowitz EA, Perkel DJ. 2009. Plastic and stable electrophysiological properties of adult avian forebrain song-control neurons across changing breeding conditions. J Neurosci. 29:6558–6567.

Miller JS, Tallarida RJ, Unterwald EM. 2009. Cocaine-induced hyperactivity and sensitization are dependent on GSK3. Neuropharmacology. 56:1116–1123.

Min R, Nevian T. 2012. Astrocyte signaling controls spike timing-dependent depression at neocortical synapses. Nat Neurosci. 15:746–753.

Mitterdorfer J, Bean BP. 2002. Potassium currents during the action potential of hippocampal CA3 neurons. J Neurosci. 22:10106–10115.

Muneer A. 2017. Wnt and GSK3 signaling pathways in bipolar disorder: clinical and therapeutic implications. Clin Psychopharmacol Neurosci. 15:100–114.

Nevian T, Sakmann B. 2006. Spine Ca2+ signaling in spike-timing-dependent plasticity. J Neurosci. 26:11001–11013.

Norris AJ, Nerbonne JM. 2010. Molecular dissection of I(A) in cortical pyramidal neurons reveals three distinct components encoded by Kv4.2, Kv4.3, and Kv1.4 alpha-subunits. J Neurosci. 30:5092–5101.

Ozaita A, Puighermanal E, Maldonado R. 2007. Regulation of PI3K/Akt/GSK-3 pathway by cannabinoids in the brain. J Neurochem. 102:1105–1114.

Pap M, Cooper GM. 1998. Role of glycogen synthase kinase-3 in the phosphatidylinositol 3-Kinase/Akt cell survival pathway. J Biol Chem. 273:19929–19932.

Pathak D, Guan D, Foehring RC. 2016. Roles of specific Kv channel types in repolarization of the action potential in genetically identified subclasses of pyramidal neurons in mouse neocortex. J Neurophysiol. 115:2317–2329.

Peineau S, Bradley C, Taghibiglou C, Doherty A, Bortolotto ZA, Wang YT, Collingridge GL. 2008. The role of GSK-3 in synaptic plasticity. Br J Pharmacol. 153(Suppl 1):S428–S437.

Peineau S, Taghibiglou C, Bradley C, Wong TP, Liu L, Lu J, Lo E, Wu D, Saule E, Bouschet T, et al. 2007. LTP inhibits LTD in the hippocampus via regulation of GSK3beta. Neuron. 53: 703–717.

Petersen CC, Crochet S. 2013. Synaptic computation and sensory processing in neocortical layer 2/3. Neuron. 78:28–48.

Ramakers GM, Storm JF. 2002. A postsynaptic transient K(+) current modulated by arachidonic acid regulates synaptic integration and threshold for LTP induction in hippocampal pyramidal cells. Proc Natl Acad Sci U S A. 99:10144–10149.

Re A, Nanni S, Aiello A, Granata S, Colussi C, Campostrini G, Spallotta F, Mattiussi S, Pantisano V, D'Angelo C, et al. 2016. Anacardic acid and thyroid hormone enhance cardiomyocytes production from undifferentiated mouse ES cells along functionally distinct pathways. Endocrine. 53: 681–688.

Rhodes KJ, Carroll KI, Sung MA, Doliveira LC, Monaghan MM, Burke SL, Strassle BW, Buchwalder L, Menegola M, Cao J, An WF, et al. 2004. KChIPs and Kv4 alpha subunits as integral components of A-type potassium channels in mammalian brain. J Neurosci. 24:7903–7915.

Rodríguez-Moreno A, Banerjee A, Paulsen O. 2010. Presynaptic NMDA receptors and spike timing-dependent depression at cortical synapses. Front Synaptic Neurosci. 17:2–18.

Rodríguez-Moreno A, Paulsen O. 2008. Spike timing-dependent long-term depression requires presynaptic NMDA receptors. Nat Neurosci. 11:744–745.

Scala F, Fusco S, Ripoli C, Piacentini R, Li Puma DD, Spinelli M, Laezza F, Grassi C, D'Ascenzo M. 2015. Intraneuronal Aβ accumulation induces hippocampal neuron hyperexcitability through A-type K(+) current inhibition mediated by activation of caspases and GSK-3. Neurobiol Aging. 36: 886–900.

Schrader LA, Birnbaum SG, Nadin BM, Ren Y, Bui D, Anderson AE, Sweatt JD. 2006. ERK/MAPK regulates the Kv4.2 potassium channel by direct phosphorylation of the pore-forming subunit. Cell Physiol. 290:852–861.

Shouval HZ, Bear MF, Cooper LN. 2002. A unified model of NMDA receptor-dependent bidirectional synaptic plasticity. Proc Natl Acad Sci U S A. 99:10831–10836.

Simons DJ, Land PW. 1987. Early experience of tactile stimulation influences organization of somatic sensory cortex. Nature. 326:694–697.

Sjöström PJ, Turrigiano GG, Nelson SB. 2003. Neocortical LTD via coincident activation of presynaptic NMDA and cannabinoid receptors. Neuron. 39:641–654.

Sánchez C, Pérez M, Avila J. 2000. GSK3beta-mediated phosphorylation of the microtubule-associated protein 2C (MAP2C) prevents microtubule bundling. Eur J Cell Biol. 79: 252–260.

Takahashi M, Tomizawa K, Kato R, Sato K, Uchida T, Fujita SC, Imahori K. 1994. Localization and developmental changes of tau protein kinase I/glycogen synthase kinase-3 beta in rat brain. J Neurochem. 63:245–255.

Takashima A, Noguchi K, Sato K, Hoshino T, Imahori K. 1993. Tau protein kinase I is essential for amyloid β-protein-induced neurotoxicity. Proc Natl Acad Sci USA. 90:7789–7793.

Tamura M, Mukai J, Gordon JA, Gogos JA. 2016. Developmental inhibition of GSK3 rescues behavioral and neurophysiological deficits in a mouse model of schizophrenia predisposition. Neuron. 89:1100–1109.

Varga AW, Yuan LL, Anderson AE, Schrader LA, Wu GY, Gatchel JR, Johnston D, Sweatt JD. 2004. Calcium-calmodulin-dependent kinase II modulates Kv4.2 channel expression and upregulates neuronal A-type potassium currents. J Neurosci. 24:3643–3654.

Wildburger NC, Laezza F. 2012. Control of neuronal ion channel function by glycogen synthase kinase-3: new prospective for an old kinase. Front Mol Neurosci. 16:5–80.

Woodgett JR. 1990. Molecular cloning and expression of glycogen synthase kinase-3/factor A. EMBO J. 9:2431–2438.

Yang L, Dan HC, Sun M, Liu Q, Sun XM, Feldman RI, Hamilton AD, Polokoff M, Nicosia SV, Herlyn M, et al. 2004. Akt/protein kinase B signaling inhibitor-2, a selective small molecule inhibitor of Akt signaling with antitumor activity in cancer cells overexpressing Akt. Cancer Res. 64:4394–4399.

Yang K, Dani JA. 2014. Dopamine D1 and D5 receptors modulate spike timing-dependent plasticity at medial perforant path to dentate granule cell synapses. J Neurosci. 34:15888–15897.

Yang F, Feng L, Zheng F, Johnson SW, Du J, Shen L, Wu CP, Lu B. 2001. GDNF acutely modulates excitability and A-type K(+) channels in midbrain dopaminergic neurons. Nat Neurosci. 4:1071–1078.

Yang YS, Kim KD, Eun SY, Jung SC. 2014. Roles of somatic A-type K(+) channels in the synaptic plasticity of hippocampal neurons. Neurosci Bull. 30:505–514.

Ye CP, Selkoe DJ, Hartley DM. 2003. Protofibrils of amyloid β-protein inhibit specific K^+ currents in neocortical cultures. Neurobiol Dis. 13:177–190.

Yu SP, Farhangrazi ZS, Ying HS, Yeh CH, Choi DW. 1998. Enhancement of outward potassium current may participate in beta-amyloid peptide-induced cortical neuronal death. Neurobiol Dis. 5:81–88.

Yuan W, Burkhalter A, Nerbonne JM. 2005. Functional role of the fast transient outward K+ current IA in pyramidal neurons in (rat) primary visual cortex. J Neurosci. 25:9185–9194.

Yue P, Gao L, Wang X, Ding X, Teng J. 2017. Intranasal administration of GDNF protects against neural apoptosis in a rat model of Parkinson's disease Through PI3K/Akt/GSK3β pathway. Neurochem Res. 42:1366–1374.

Zucca S, D'Urso G, Pasquale V, Vecchia D, Pica G, Bovetti S, Moretti C, Varani S, Molano-Mazon M, Chiappalone M, et al. 2017. An inhibitory gate for state transition in cortex. Elife. 6: e26177.